

## Growth of gallium nitride and indium nitride nanowires on conductive and flexible carbon cloth substrates†

Cite this: *Nanoscale*, 2013, 5, 1820

Yi Yang,<sup>‡a</sup> Yichuan Ling,<sup>‡a</sup> Gongming Wang,<sup>a</sup> Xihong Lu,<sup>ab</sup> Yexiang Tong<sup>b</sup> and Yat Li<sup>\*a</sup>

Received 20th December 2012

Accepted 16th January 2013

DOI: 10.1039/c3nr34200j

[www.rsc.org/nanoscale](http://www.rsc.org/nanoscale)

We report a general strategy for synthesis of gallium nitride (GaN) and indium nitride (InN) nanowires on conductive and flexible carbon cloth substrates. GaN and InN nanowires were prepared via a nanocluster-mediated growth method using a home built chemical vapor deposition (CVD) system with Ga and In metals as group III precursors and ammonia as a group V precursor. Electron microscopy studies reveal that the group III-nitride nanowires are single crystalline wurtzite structures. The morphology, density and growth mechanism of these nanowires are determined by the growth temperature. Importantly, a photoelectrode fabricated by contacting the GaN nanowires through a carbon cloth substrate shows pronounced photoactivity for photoelectrochemical water oxidation. The ability to synthesize group III-nitride nanowires on conductive and flexible substrates should open up new opportunities for nanoscale photonic, electronic and electrochemical devices.

Semiconductor nanowires have been extensively studied as versatile building blocks for active nanoscale electronic and photonic devices.<sup>1–4</sup> Among them, group III-nitride<sup>5–8</sup> nanomaterials have demonstrated great potential in device applications, including field-effect transistors,<sup>9–11</sup> light-emitting diodes,<sup>12–16</sup> and lasers.<sup>17–22</sup> For practical applications, it is highly desirable to have a high density of nanowires assembled on a conductive, flexible and low-cost substrate that connects all the nanowires to form scalable and wearable electronic and photonic devices. Synthesis of group III-nitride nanowires has been demonstrated on a variety of sapphire substrates.<sup>5</sup> Yang and coworkers also reported the growth of high density vertically aligned GaN nanowire arrays on  $\gamma$ -LiAlO<sub>2</sub> and MgO

substrates.<sup>23</sup> While sapphires are the most commonly used substrates, they are not conductive, which restricted the applications of the group III-nitride nanodevices. To address this problem, considerable efforts have been placed over the past few years in preparing group III-nitride nanowires on conductive substrates such as silicon,<sup>24,25</sup> ZrB<sub>2</sub>,<sup>26</sup> (Mn,Zn)Fe<sub>2</sub>O<sub>4</sub>,<sup>27</sup> SiC,<sup>28</sup> and stainless steel.<sup>29</sup> However, these substrates are either expensive or not flexible. Carbon cloth substrates have been extensively used as electrode materials in applications such as fuel cells and supercapacitors due to their low cost, excellent conductivity, corrosion resistance, and flexibility.<sup>30–33</sup> These works motivated us to explore the potential of the carbon cloth as a growth substrate for group III-nitride materials, which could potentially address the limitation of conventional substrates. Here we report, for the first time, the high yield synthesis of GaN and InN nanowires on carbon cloth substrates using the chemical vapor deposition (CVD) method. Importantly, we demonstrated that GaN nanowire arrays grown on the conductive carbon cloth substrate can serve as a photoelectrode for photoelectrochemical water oxidation.

GaN nanowires were synthesized on a ZnO seeded carbon cloth substrate in a hydrogen atmosphere by the CVD method (Fig. 1), using gallium metal and ammonia as Ga and N precursors, respectively (Experimental section, ESI†). Nickel(II) nitrate [Ni(NO<sub>3</sub>)<sub>2</sub>] was used as a catalyst for the growth. We obtained high yield GaN nanowires in a range of temperatures between 900 and 1000 °C (Fig. S1, ESI†). Scanning electron microscopy (SEM) images show that the nanowire morphology and size are closely associated with the growth temperatures (Fig. 2). As shown in Fig. 2a and e, nanowires synthesized at 800 °C exhibit a broad distribution of the wire diameter. These nanowires are thin and kinked, with a typical diameter of less than 50 nm and the length in the range of 1 to 4  $\mu$ m. When the growth temperature increased to 900 °C, straight nanowires with uniform diameter were obtained (Fig. 2b and f). These nanowires have a typical length in the range of 2 to 5  $\mu$ m, slightly longer than the wires obtained at 800 °C. Importantly, nanoparticles were observed on the tips of nanowires obtained

<sup>a</sup>Department of Chemistry and Biochemistry, University of California, Santa Cruz, California 95064, USA. E-mail: [yli@chemistry.ucsc.edu](mailto:yli@chemistry.ucsc.edu)

<sup>b</sup>KLGHEI of Environment and Energy Chemistry, MOE of the Key Laboratory of Bioinorganic and Synthetic Chemistry, School of Chemistry and Chemical Engineering, Sun Yat-Sen University, Guangzhou 510275, People's Republic of China

† Electronic supplementary information (ESI) available. See DOI: 10.1039/c3nr34200j

‡ These authors contributed equally to this work.

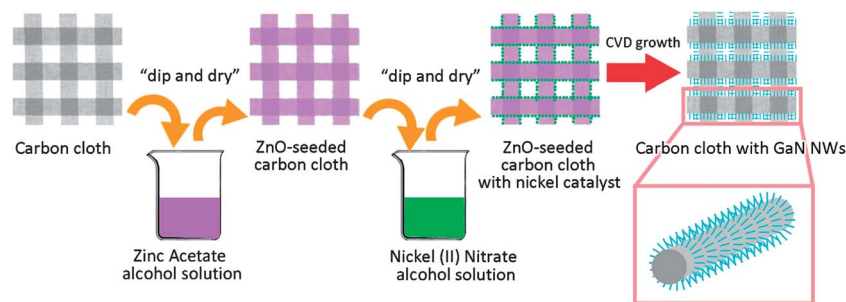


**Fig. 1** Schematic diagram illustrating the growth procedure for GaN nanowires on a carbon cloth substrate.

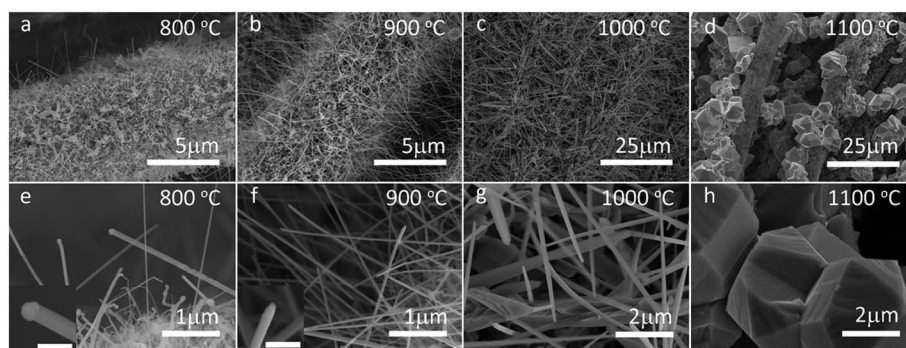


**Fig. 2** SEM images collected for the GaN nanowires prepared at different growth temperatures. Insets in (e) and (f) show the SEM images collected at the tip of GaN nanowires obtained at 800 and 900 °C. Scale bars in insets are 200 nm.

at 800 and 900 °C, suggesting a vapor–liquid–solid (VLS) growth process.<sup>34,35</sup> When the growth temperature further increased to 1000 °C (Fig. 2c and g), the nanowires became even thicker and longer, with a typical length of 6 to 25 μm. It is noteworthy that nanoparticles were not observed on the tips of nanowires obtained at 1000 °C, indicating that the nanowire growth mechanism changed as the temperature increases from 900 to 1000 °C. At 1100 °C, the anisotropic growth of the 1D structure is no longer favorable and the formation of microcrystals was observed.

Powder X-ray diffraction spectra were collected for nanowires grown at 900 °C and 1000 °C (denoted as GaN-900 and GaN-1000), and were compared to those obtained for a blank carbon cloth substrate treated under the same growth conditions in the absence of a Ga metal precursor (Fig. 3a). The dashed lines highlight the peaks that can be indexed to the wurtzite GaN structure (PDF # 65-3410). These sharp diffraction peaks suggest the good crystallinity of GaN nanowires. We also observed the diffraction peaks that can be indexed to the Ga metal, which could be deposited on the substrate during the CVD growth process. GaN-900 and GaN-1000 nanowires show distinct size distribution. Diameter histograms were collected for GaN-900 (Fig. 3b) and GaN-1000 (Fig. 3c) nanowires based on the 150 nanowires we studied by SEM analysis. The Gaussian fittings based on these histograms revealed that the average diameters of GaN-900 and GaN-1000 nanowires are around 50 nm and 200 nm, respectively.

TEM analyses were used to further characterize the structure and the growth mechanism of GaN-900 and GaN-1000

nanowires. The TEM image collected for the GaN-900 nanowire showed that the nanowire diameter is essentially the same as the diameter of the Ni nanocluster, as expected for the VLS process (Fig. 4a).<sup>34</sup> The lattice spacing of the catalyst was measured to be 0.20 nm, consistent with the *d*-spacing of the Ni (111) plane (Fig. 4c). The homogeneous contrast along the wire suggests that the nanowire is a single crystalline material. The HRTEM image revealed the lattice fringes with interplanar spacings of 0.25 and 0.24 nm, corresponding to the (002) and (101) planes of wurtzite GaN, respectively. The angles between these lattice planes and the lattice plane perpendicular to the nanowire growth axis are 90° and 28.05°, suggesting that the GaN-900 nanowire grew along the [100] direction. Furthermore, the TEM image shows that the GaN-1000 nanowire is a single-crystal with a smooth surface and a sharp nanowire end (Fig. 4b). Interestingly, we did not observe any Ni catalyst for all the GaN-1000 nanowires we studied. The absence of a catalyst indicates that the growth of the GaN-1000 nanowires could be governed by a self-catalytic vapor–solid process<sup>36</sup> or a defect induced growth mechanism,<sup>37</sup> instead of the VLS mechanism observed for GaN-900 nanowires. The TEM image also reveals that the lattice fringes that are perpendicular to the nanowire growth axis have an interplanar spacing of 0.28 nm, which is consistent with the wurtzite GaN (100) plane and therefore confirms that the GaN-1000 nanowires also grew along the [100] direction.

Furthermore, we found that the ZnO seeds also play an important role in the VLS growth of GaN-900 nanowires. Fig. S2 (ESI†) shows the SEM images collected for GaN nanowires

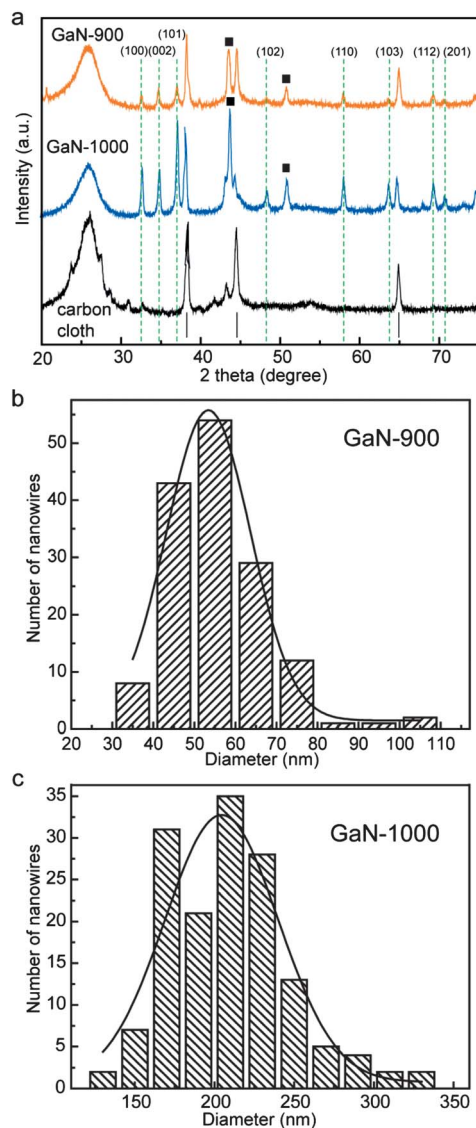


**Fig. 3** (a) XRD spectra collected for GaN-900 and GaN-1000 nanowires grown on a carbon cloth substrate as well as on a blank carbon cloth substrate. Dashed lines highlight the characteristic diffraction peaks of wurtzite GaN. Solid lines highlight the diffraction peaks for the Al substrate. Solid squares highlight the diffraction peaks for Ga metal. (b and c) Diameter histograms collected for 150 GaN-900 and GaN-1000 nanowires. The solid lines are the Gaussian fittings.

grown on a carbon cloth substrate without ZnO coating. While nanowires were still obtained in the growth temperature window between 800 and 1000 °C, the density of GaN nanowires obtained at 800 and 900 °C was substantially lower than that obtained on the ZnO seeded substrate at the same temperatures. Additionally, most of these GaN nanowires are severely twisted, which is different from the straight nanowires observed on the ZnO seeded substrate. Ni catalysts were found at the tip of these nanowires. Meanwhile, the morphology and density of GaN nanowires prepared at 1000 °C are similar to the GaN-1000 nanowires. These results suggest that the ZnO seeds could facilitate the VLS growth of GaN nanowires at a temperature of 900 °C or below, by providing a single crystal substrate/crystal facets for GaN nanowire growth.

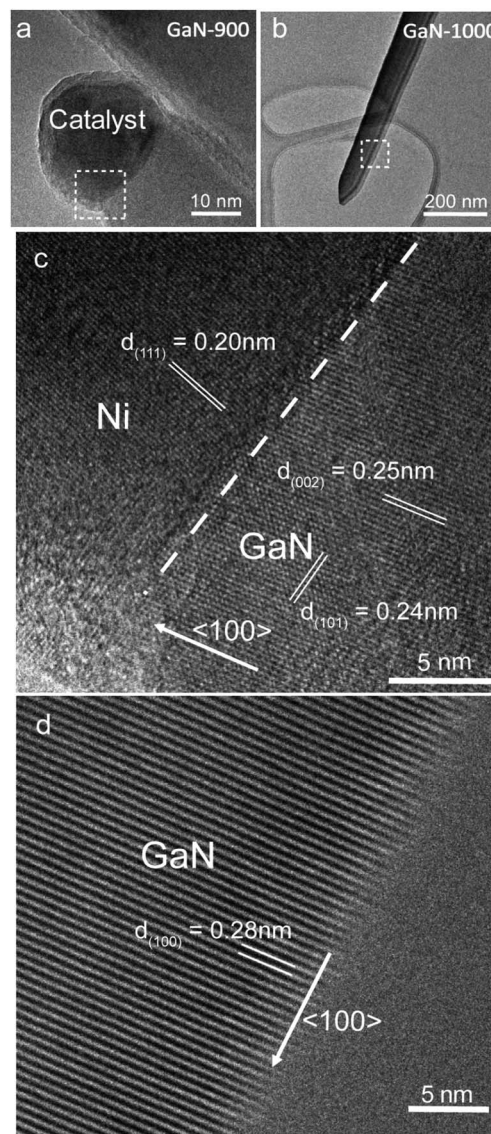


**Fig. 4** TEM images of (a) GaN-900 and (b) GaN-1000 nanowires. (c) Lattice-resolved TEM images recorded at (c) the interface of the GaN-900 nanowire and nickel catalyst, and (d) the edge of GaN-1000 nanowire, highlighted by the dashed boxes in (a) and (b).

We further extended this growth approach to prepare another important group III-nitride material, InN nanowires, on the carbon cloth substrate. As shown in Fig. 5a, the carbon fibers were uniformly covered by InN nanowires, which have lengths between 500 nm and 2 μm. A diameter histogram was plotted for the 150 InN nanowires we studied (Fig. 5d). These nanowires exhibit uniform diameters, with an average diameter of 40 nm. Individual InN nanowires were further characterized with TEM. As shown in Fig. 5b, a gold nanoparticle was found on the tip of the InN nanowire. It indicates that the InN growth is also governed by the VLS process. The lattice-resolved TEM image was collected at the interface between a gold nanoparticle and an InN nanowire. The interplanar spacings in the nanowire and the particle were measured to be 0.283 nm and 0.235 nm, corresponding to the wurtzite InN (002) plane and gold (111)



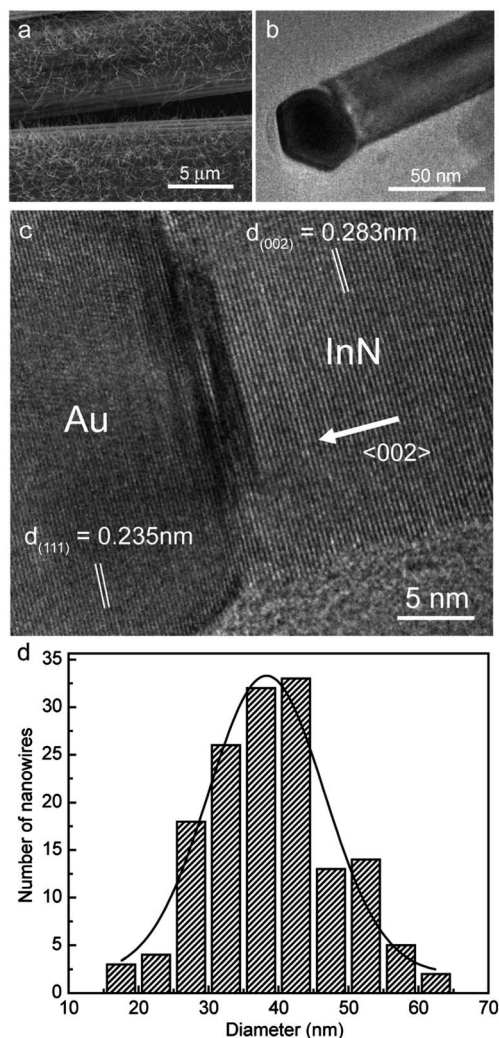


**Fig. 5** (a) SEM image of InN nanowires on a carbon cloth substrate. (b) TEM image of the InN nanowire. (c) Lattice-resolved TEM image collected at the interface between a gold nanoparticle and InN nanowire. (d) Diameter histogram collected for 150 InN nanowires. The solid line is the Gaussian fitting.

plane, respectively. Additionally, the InN (002) plane is perpendicular to the nanowire growth axis, indicating that the InN nanowire grew along the [002] direction.

The capability of growing group III-nitride nanowires on a flexible conducting substrate could open up new opportunities for device fabrication and applications. Here we exemplified this idea by employing Si-doped GaN nanowire arrays grown on a carbon cloth as a photoelectrode for photoelectrochemical water oxidation. GaN has been studied for photocatalytic water splitting applications because of its favorable band edge position, in which the conduction band and valence band straddle the hydrogen reduction ( $\text{H}^+/\text{H}_2$ ) and water oxidation ( $\text{H}_2\text{O}/\text{O}_2$ ) potentials.<sup>38,39</sup> Silicon is known to be a shallow donor that can increase the electrical conductivity of GaN nanowires,<sup>40</sup> which is important for a photoelectrode. Si-doped GaN nanowires were prepared on a carbon cloth substrate using the same conditions for GaN-1000 nanowires, with the addition of diluted silane gas (100 ppm in ultrahigh purity hydrogen) flowing at a rate of

5 sccm during the growth. Photoelectrochemical measurements were performed in a three-electrode system, using the nanowire-arrayed electrode as the working electrode, platinum sheet and Ag/AgCl (saturated KCl) as the counter and the reference electrodes, respectively. 0.5 M  $\text{Na}_2\text{SO}_4$  solution (pH = 7) was used as an electrolyte because photoanodic etching of GaN could occur in both strong basic and acidic electrolytes.<sup>41</sup> The photoactivity of the nanowire electrode was measured under the simulated solar illumination at  $100 \text{ mW cm}^{-2}$ . Fig. 6a shows the linear sweep voltammogram collected for the Si-doped GaN-1000 nanowire electrode with light on-off cycles in a potential range of  $-0.1$  to  $0.9 \text{ V vs. Ag/AgCl}$ . The results confirmed that these GaN nanowires exhibit pronounced photoresponse under white light illumination. To examine the photostability of GaN nanowires for water oxidation,  $I$ - $t$  curves were collected at  $0.7 \text{ V vs. Ag/AgCl}$  with light on-off cycles at  $100 \text{ mW cm}^{-2}$  (Fig. 6b). We observed that the photocurrent density slightly decays from  $31$  to  $25 \mu\text{A cm}^{-2}$  after  $3600 \text{ s}$ , indicating that the Si-doped GaN nanowire photoanode was relatively stable for photoelectrochemical water oxidation.

In summary, we have reported a simple method to prepare high yield GaN and InN nanowires on low cost, conductive and flexible carbon cloth substrates. The densities, lengths and diameters of nanowires can be controlled by adjusting growth temperatures. The Si-doped GaN nanowires grown on the carbon cloth can serve as a photoanode for photoelectrochemical water oxidation. These electrodes showed

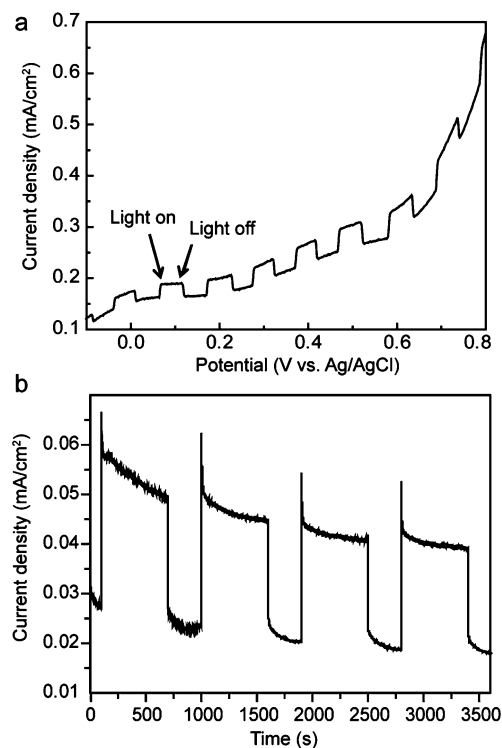


**Fig. 6** (a) Linear sweep voltammogram collected for Si-doped GaN-1000 nanowires on a carbon cloth under light illumination ( $100 \text{ mW cm}^{-2}$ , AM 1.5 G). (b)  $I$ - $t$  curves recorded for the nanowire photoelectrode at  $0.7 \text{ V vs. Ag/AgCl}$  for  $3600 \text{ s}$ .

pronounced photoactivities. Carbon cloth serves as a promising conductive and flexible substrate for group-III nitride nanomaterials, which could open up new opportunities for nanoscale photonic, electronic and electrochemical devices.

## Acknowledgements

Y.L. acknowledges the financial support of United States NSF CAREER award (DMR-0847786). The TEM works were performed at NCEM at Lawrence Berkeley National Laboratory, which are supported by the Office of Science, Office of Basic Energy Sciences of the U.S. Department of Energy under contract no. DE-AC02-05CH11231. G.W. acknowledges the financial support of Chancellor's Dissertation Year Fellowship at University of California, Santa Cruz. Y.X.T. acknowledges the financial support by the Natural Science Foundations of China (21273290) and the Research Fund for the Doctoral Program of Higher Education of China (no. 20120171110043). X.L. thanks the Academic New Artist Ministry of Education Doctoral Post Graduate (China) and China Scholarship Council for financial support.

## References

- 1 C. M. Lieber, *MRS Bull.*, 2003, **28**, 486–491.
- 2 Y. Li, F. Qian, J. Xiang and C. M. Lieber, *Mater. Today*, 2006, **9**, 18–27.
- 3 X. C. Jiang, Q. H. Xiong, S. Nam, F. Qian, Y. Li and C. M. Lieber, *Nano Lett.*, 2007, **7**, 3214–3218.
- 4 L. S. Li, Y. H. Yu, F. Meng, Y. Z. Tan, R. J. Hamers and S. Jin, *Nano Lett.*, 2012, **12**, 724–731.
- 5 O. Ambacher, *J. Phys. D: Appl. Phys.*, 1998, **31**, 2653–2710.
- 6 S. K. Lim, M. Brewster, F. Qian, Y. Li, C. M. Lieber and S. Gradecak, *Nano Lett.*, 2009, **9**, 3940–3944.
- 7 S. A. Dayeh, C. Soci, X. Y. Bao and D. L. Wang, *Nano Today*, 2009, **4**, 347–358.
- 8 Y. J. Dong, B. Z. Tian, T. J. Kempa and C. M. Lieber, *Nano Lett.*, 2009, **9**, 2183–2187.
- 9 Y. Li, J. Xiang, F. Qian, S. Gradecak, Y. Wu, H. Yan, H. Yan, D. A. Blom and C. M. Lieber, *Nano Lett.*, 2006, **6**, 1468–1473.
- 10 M. Azize, A. L. Hsu, O. I. Saadat, M. Smith, X. Gao, S. P. Guo, S. Gradecak and T. Palacios, *IEEE Electron Device Lett.*, 2011, **32**, 1680–1682.
- 11 S. A. Dayeh, D. Susac, K. L. Kavanagh, E. T. Yu and D. Wang, *Nano Lett.*, 2008, **8**, 3114–3119.
- 12 X. F. Duan, Y. Huang, Y. Cui, J. F. Wang and C. M. Lieber, *Nature*, 2001, **409**, 66–69.
- 13 Z. H. Zhong, F. Qian, D. L. Wang and C. M. Lieber, *Nano Lett.*, 2003, **3**, 343–346.
- 14 H. M. Kim, Y. H. Cho, H. Lee, S. I. Kim, S. R. Ryu, D. Y. Kim, T. W. Kang and K. S. Chung, *Nano Lett.*, 2004, **4**, 1059–1062.
- 15 F. Qian, Y. Li, S. Gradecak, D. L. Wang, C. J. Barrelet and C. M. Lieber, *Nano Lett.*, 2004, **4**, 1975–1979.
- 16 Y. Huang, X. F. Duan and C. M. Lieber, *Small*, 2005, **1**, 142–147.
- 17 M. H. Huang, S. Mao, H. Feick, H. Q. Yan, Y. Y. Wu, H. Kind, E. Weber, R. Russo and P. D. Yang, *Science*, 2001, **292**, 1897–1899.
- 18 J. C. Johnson, H. J. Choi, K. P. Knutsen, R. D. Schaller, P. D. Yang and R. J. Saykally, *Nat. Mater.*, 2002, **1**, 106–110.
- 19 X. F. Duan, Y. Huang, R. Agarwal and C. M. Lieber, *Nature*, 2003, **421**, 241–245.
- 20 R. Agarwal, C. J. Barrelet and C. M. Lieber, *Nano Lett.*, 2005, **5**, 917–920.
- 21 F. Qian, Y. Li, S. Gradecak, H. G. Park, Y. J. Dong, Y. Ding, Z. L. Wang and C. M. Lieber, *Nat. Mater.*, 2008, **7**, 701–706.
- 22 F. Qian, M. Brewster, S. K. Lim, Y. C. Ling, C. Greene, O. Laboutin, J. W. Johnson, S. Gradecak, Y. Cao and Y. Li, *Nano Lett.*, 2012, **12**, 3344–3350.
- 23 T. Kuykendall, P. J. Pauzauskie, Y. F. Zhang, J. Goldberger, D. Sirbully, J. Denlinger and P. D. Yang, *Nat. Mater.*, 2004, **3**, 524–528.
- 24 S. H. Lee, Y. H. Mo, K. S. Nahm, E. K. Suh and K. Y. Lim, *Phys. Status Solidi C*, 2002, **0**, 148–151.
- 25 W. Guo, M. Zhang, P. Bhattacharya and J. Heo, *Nano Lett.*, 2011, **11**, 1434–1438.
- 26 Y. Tomida, S. Nitta, S. Kamiyama, H. Amano, I. Akasaki, S. Otani, H. Kinoshita, R. Liu, A. Bell and F. A. Ponce, *Appl. Surf. Sci.*, 2003, **216**, 502–507.
- 27 J. Ohta, H. Fujioka and M. Oshima, *Appl. Phys. Lett.*, 2003, **83**, 3060–3062.
- 28 J. R. LaRoche, B. Luo, F. Ren, K. H. Baik, D. Stodilka, B. Gila, C. R. Abernathy, S. J. Pearton, A. Usikov, D. Tsvetkov, V. Soukhoveev, G. Gainer, A. Rechnikov, V. Dimitriev, G. T. Chen, C. C. Pan and J. I. Chyi, *Solid-State Electron.*, 2004, **48**, 193–196.
- 29 C. Pendyala, J. B. Jasins, J. H. Kim, V. K. Vendra, S. Lisenkov, M. Menon and M. K. Sunkara, *Nanoscale*, 2012, **4**, 6269–6275.
- 30 S. H. Jo, D. Z. Wang, J. Y. Huang, W. Z. Li, K. Kempa and Z. F. Ren, *Appl. Phys. Lett.*, 2004, **85**, 810–812.
- 31 X. H. Zhang, L. Gong, K. Liu, Y. Z. Cao, X. Xiao, W. M. Sun, X. J. Hu, Y. H. Gao, J. A. Chen, J. Zhou and Z. L. Wang, *Adv. Mater.*, 2010, **22**, 5292–5296.
- 32 Q. Cheng, J. Tang, J. Ma, H. Zhang, N. Shinya and L. C. Qin, *J. Phys. Chem. C*, 2011, **115**, 23584–23590.
- 33 G. Wang, X. Lu, Y. Ling, T. Zhai, H. Wang, Y. Tong and Y. Li, *ACS Nano*, 2012, **6**, 10296–10302.
- 34 X. F. Duan and C. M. Lieber, *J. Am. Chem. Soc.*, 2000, **122**, 188–189.
- 35 T. Kuykendall, P. Pauzauskie, S. K. Lee, Y. F. Zhang, J. Goldberger and P. D. Yang, *Nano Lett.*, 2003, **3**, 1063–1066.
- 36 C. Liu, Z. Hu, Q. Wu, X. Z. Wang, Y. Chen, H. Sang, J. M. Zhu, S. Z. Deng and N. S. Xu, *J. Am. Chem. Soc.*, 2005, **127**, 1318–1322.
- 37 Z. Chen, C. B. Cao and H. S. Zhu, *J. Phys. Chem. C*, 2007, **111**, 1895–1899.
- 38 H. S. Jung, Y. J. Hong, Y. Li, J. Cho, Y. J. Kim and G. C. Yi, *ACS Nano*, 2008, **2**, 637–642.
- 39 D. F. Wang, A. Pierre, M. G. Kibria, K. Cui, X. G. Han, K. H. Bevan, H. Guo, S. Paradis, A. R. Hakima and Z. T. Mi, *Nano Lett.*, 2011, **11**, 2353–2357.
- 40 W. Gotz, N. M. Johnson, C. Chen, H. Liu, C. Kuo and W. Imler, *Appl. Phys. Lett.*, 1996, **68**, 3144–3146.
- 41 I. M. Huygens, K. Strubbe and W. P. Gomes, *J. Electrochem. Soc.*, 2000, **147**, 1797–1802.